Front. Environ. Sci. Eng. 2021, 15(4): 78
https://doi.org/10.1007/s11783-020-1371-5

RESEARCH ARTICLE

Optimization of the O_3/H_2O_2 process with response surface methodology for pretreatment of mother liquor of gas field wastewater

Haoran Feng, Min Liu, Wei Zeng, Ying Chen (✉)

College of Architecture and Environment, Sichuan University, Chengdu 610065, China

HIGHLIGHTS

- Real ML-GFW with high salinity and high organics was degraded by O_3/H_2O_2 process.
- Successful optimization of operation conditions was attained using RSM based on CCD.
- Single-factor experiments in advance ensured optimal experimental conditions.
- The satisfactory removal efficiency of TOC was achieved in spite of high salinity.
- The initial pH plays the most significant role in the degradation of ML-GFW.

GRAPHIC ABSTRACT

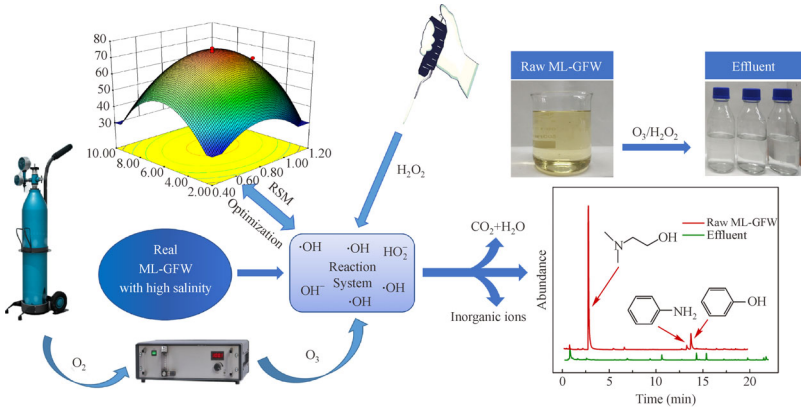

ARTICLE INFO

Article history:
Received 3 June 2020
Revised 26 October 2020
Accepted 27 October 2020
Available online 30 November 2020

Keywords:
High salinity
High organic matters
Gas field wastewater
O_3/H_2O_2
Response surface methodology

ABSTRACT

The present study reports the use of the O_3/H_2O_2 process in the pretreatment of the mother liquor of gas field wastewater (ML-GFW), obtained from the multi-effect distillation treatment of the gas field wastewater. The range of optimal operation conditions was obtained by single-factor experiments. Response surface methodology (RSM) based on the central composite design (CCD) was used for the optimization procedure. A regression model with Total organic carbon (TOC) removal efficiency as the response value was established (R^2 = 0.9865). The three key factors were arranged according to their significance as: pH>H_2O_2 dosage>ozone flow rate. The model predicted that the best operation conditions could be obtained at a pH of 10.9, an ozone flow rate of 0.8 L/min, and H_2O_2 dosage of 6.2 mL. The dosing ratio of ozone was calculated to be 9.84 mg O_3/mg TOC. The maximum removal efficiency predicted was 75.9%, while the measured value was 72.3%. The relative deviation was found to be in an acceptable range. The ozone utilization and free radical quenching experiments showed that the addition of H_2O_2 promoted the decomposition of ozone to produce hydroxyl radicals (·OH). This also improved the ozone utilization efficiency. Gas chromatography-mass spectrometry (GC-MS) analysis showed that most of the organic matters in ML-GFW were degraded, while some residuals needed further treatment. This study provided the data and the necessary technical supports for further research on the treatment of ML-GFW.

1 Introduction

China is rich in several energy resources. Wu et al. (2016) and Dai et al. (2018) have reported that the Sichuan Basin in China has abundant natural gas reserves and shows broad prospects for development. Ozgun et al. (2013) have

✉ Corresponding author
E-mail: cylm@163.com

reported that wastewater produced during gas production threatens the ecological system. A proper treatment procedure is hence needed to protect the environment against the hazards of the gas field wastewater.

Several physical and physical-chemical methods are usually applied to treat gas field wastewater. It is necessary to recover beneficial resources from wastewater as much as possible to reduce environmental damage. At present, one of the possible strategies to achieve this is to use cryogenic multi-effect distillation method, as suggested by Yang and Xiang (2018). This method can not only improve the water quality of the condensate to the reuse standard but can also recover the salt. Nevertheless, Wang et al. (2019b) reported that cryogenic multi-effect distillation process produces the mother liquor of gas field wastewater (ML-GFW), a concentrated liquid with high salinity and high organic matter, which is hard to treat.

Ozgun et al. (2013) reported that the high salinity and toxicity of wastewater inhibits the growth of microorganisms, restricting the use of bio-techniques. Researchers have recently found out that advanced oxidation processes (AOPs) could be a beneficial tool for enhancing the treatment processes. According to Malik et al. (2020), AOPs could accelerate the degradation of organic contaminants by generating hydroxyl radicals (·OH) with oxidation potential as high as 2.80 V. AOPs include the usage of Ozone (O_3), Hydrogen peroxide (H_2O_2), Fenton, UV (Ultraviolet), and other combined processes, such as O_3/H_2O_2, UV/H_2O_2, and $UV/O_3/H_2O_2$. A combined process could be a better choice for wastewater treatment because of the higher organic matter content in ML-GFW. Lu et al. (2019) successfully applied UV/O_3 process to degrade the evaporative condensing liquid of gas field wastewater and achieved ideal performance. However, due to the poor light transmittance of ML-GFW, the use of AOPs with UV method is unsuitable. Wang et al. (2019b) pretreated ML-GFW with the electro-Fenton process. However, Moradi et al. (2020) reported the disadvantages of this process, such as plate passivation and short electrode life.

H_2O_2 being a green and efficient oxidizer, O_3/H_2O_2 process has been widely applied to the treatment of industrial wastewater (Wen et al., 2011; Oh et al., 2014; Li et al., 2015) but its applicability in gas field wastewater remains unexplored. It has been reported by Barndõk et al. (2012) that the high salinity of the water has a limited effect on ozonation, thereby showing the potential of O_3/H_2O_2 process in treating ML-GFW.

The treatment performance can be improved by maintaining proper operating conditions. Response surface methodology (RSM) is a reliable analytical method to effectively analyze the influence of various parameters and to study the effect of these parameters on the reaction process. This methodology uses the minimum number of experiments possible to obtain the optimal conditions (Karimifard and Moghaddam, 2018). Recently, RSM has been introduced in the field of sewage treatment to optimize the operation conditions (Cristóvão et al., 2015; Sonwani et al., 2019; Wang et al., 2019a; Yazici Guvenc and Varank, 2021).

In this study, O_3/H_2O_2 process was used to pretreat ML-GFW. The single-factor experiments over the possible influencing factors were carried out to determine the corresponding changes and the optimal ranges. Based on the experimental data, the operation conditions were optimized and verified by RSM. To study the degradation mechanism of organic matter, the ozone utilization experiment and the hydroxyl radical quenching experiment were carried out. The organic compounds in ML-GFW were also analyzed by GC-MS.

2 Materials and methods

2.1 Materials

ML-GFW used in this study was collected from a gas field in Sichuan province, China. The primary characteristics of ML-GFW were measured as follows. The pH of raw ML-GFW was 9.7, the concentration of chemical oxygen demand (COD) was (1.23–1.24) $\times$ 10^4 mg/L, the concentration of total organic carbon (TOC) was (1.88–1.89) $\times$ 10^3 mg/L, and the concentration of chloride ion (Cl^-) was (2.01–2.02) $\times$ 10^2 g/L.

Analytical grade (AR) of H_2SO_4, NaOH, 30% H_2O_2, KI, tert-butanol (TBA), $AgNO_3$, and K_2CrO_4 were purchased from the Kelong Chemical Reagent Plant (Chengdu, China). Analytical grade (AR) of $Na_2S_2O_3$ was purchased from the Shanghai Aladdin Bio-Chem Technology Co., Ltd. (Shanghai, China). Industrial grade oxygen (99% pure) was supplied by Sichuan Qiaoyuan Gas Co., Ltd. (Chengdu, China). Ultrapure water was produced by UPK-I-5 (Ulupure, China), used to prepare solutions for the experiments.

2.2 Single-factor experiments

Figure 1 presents the experimental set-up in this study. The total volume of the reactor was 500 mL, with an effective volume of 300 mL. Ozone was generated by an ozonator (COM-AD-01, Anseros, Germany) using pure oxygen as the source then introduced into the reactor via a microporous aerator. The ozone flow rate was regulated in the range of 0.6–1.4 L/min by a pressure valve. A certain dosage of H_2O_2 was added at the beginning of the reaction. KI solution (2%) was used to absorb the tail gas. The pH value of the reaction system was adjusted by H_2SO_4 (50%) and NaOH (30%). The reaction temperature was controlled at 25°C via a constant temperature water bath.

In this study, single-factor experiments were carried out by varying the parameters: reaction time (1, 2, 3, 4, 5 and 6 h), pH (4, 6, 8, 9.7 and 12), ozone flow rate (0.6, 0.8, 1.0,

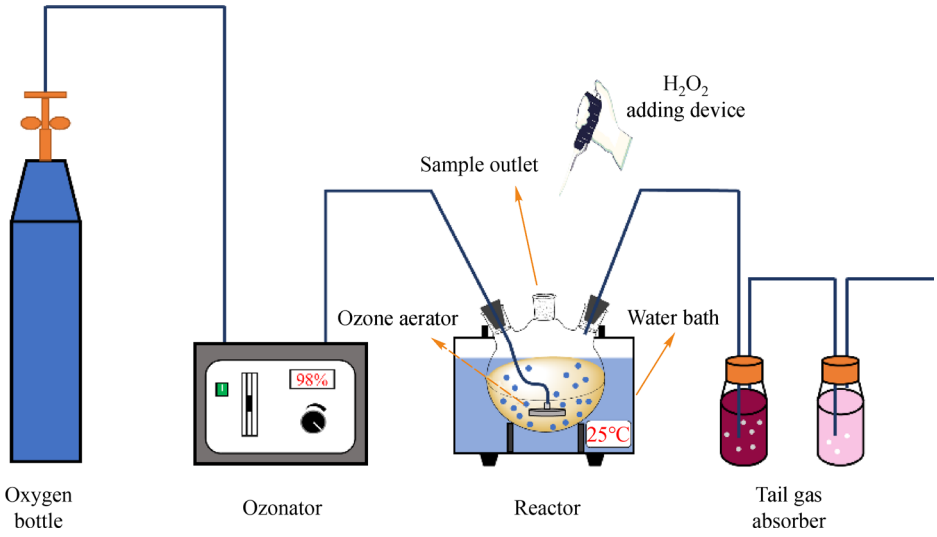

Fig. 1 Schematic representation of the O_3/H_2O_2 system.

1.2 and 1.4 L/min) and dosage of H_2O_2 (2, 4, 6, 8 and 10 mL), respectively.

Three parallel experiments were conducted for each batch, and the average values were calculated to get the final values.

2.3 RSM optimization experiments

Single-factor experiments were used to determine the significant factors and their optimum ranges. A set of tests with central composite design (CCD) based on the optimal parameters obtained from the single-factor experiments were performed to improve the performance using RSM.

The results can be fit to a second-order polynomial model with Design-expert 8.0.5, as shown in Eq. (1) (Sonwani et al., 2019). The model can predict the optimal operation conditions based on a verification experiment. The validity of the model can be determined by comparing and analyzing the actual and predicted values.

$$Y = \hat{a}_0 + \hat{a}_i X_i + \hat{a}_j X_j + \hat{a}_{ij} X_{ij} + \hat{a}_{ii} X_i^2 + \hat{a}_{jj} X_j^2 + \ldots, \quad (1)$$

where Y represents the response value, $\hat{a}$ represents the correlation coefficient, i and j represent the coefficients of linear multi-degree.

A certain dose of H_2O_2 was divided into two parts on average and added at the beginning (0 min) and halfway (90 min) of the reaction in the RSM experiments. Three parallel experiments were performed for each operation condition to ensure the accuracy of the results.

2.4 Mechanism verification experiments

To study the mechanism of the process, an ozone utilization experiment and a hydroxyl radical quenching experiment were designed.

The ozone utilization experiment was performed in two different ways. One group was treated only with ozone, while extra H_2O_2 was added to the other group. All other factors were kept constant in both groups. The consumption of ozone was calculated for both groups.

TBA (15 mmol/L) was added to the reactor to quench the hydroxyl radicals under the optimal conditions predicted by RSM. The removal efficiency of organic matter was subsequently investigated.

2.5 Analytical methods

The pH value of samples was tested by a pH meter (pHB-4, Leici, China).

The high salinity of ML-GFW can seriously affect the COD test and lead to a misalignment. Therefore, TOC was used to characterize the organic matter content in this study. The results were analyzed by LAR Quick TOC (Germany). During the experiment, 3 mL of ML-GFW was taken from the reaction system at a predetermined time interval and then filtered through a 0.45 μm microporous membrane. The removal efficiency of TOC (%) was calculated by Eq. (2).

$$\text{The removal efficiency of TOC}(\%) = \frac{\text{TOC}_0 - \text{TOC}_t}{\text{TOC}_0} \times 100, \quad (2)$$

where TOC_0 represents the TOC concentration of raw ML-GFW and TOC_t represents the TOC concentration after treatment by O_3/H_2O_2.

The KI adsorption method was used to determine the concentration of ozone (Fu et al., 2018; Lu et al., 2019). The ozone produced by the ozonator was directly absorbed by the KI solution (2%), which was defined as the total

amount of ozone. The unreacted ozone after oxidation was fed to the tail gas absorber filled with KI solution. This represented the amount of unreacted ozone. The standard solution of $Na_2S_2O_3$ (0.1 mol/L) was used to titrate iodine (I_2) produced in the reaction. The ozone concentration was calculated, and the utilization rate of ozone (%) was determined per Eq. (3).

$$\text{Ozone utilization rate}(\%) = \frac{(O_3)_0 - (O_3)_t}{(O_3)_0} \times 100, \quad (3)$$

where $(O_3)_0$ and $(O_3)_t$ represent the total amount of ozone and the amount of unreacted ozone, respectively.

GC-MS (GCMS-QP2010 Plus, Shimadzu, Japan) was used to analyze the changes in organic matter in ML-GFW, detected by Analytical & Testing Center, Sichuan University, China. The parameters used in the test were taken from Lu et al. (2019). The modified heating conditions were as follows: 40°C for 5 min, 120°C for 1 min with a rising rate of 5°C/min, and 290°C for 5 min with an increasing rate of 10°C/min. The full scan mode ranged from 33 to 500 amu. The NIST database was utilized for a retrieval process.

The concentration of chloride ion was detected by $AgNO_3$ titration (GB/T 15453–2018).

3 Results and discussion

3.1 Single-factor experiments

3.1.1 Effects of reaction time

Reaction time is one of the critical factors affecting the removal efficiency of pollutants. Appropriate reaction time can not only maximize the removal efficiency of pollutants but also effectively reduce the operation costs. The effects of reaction time on the TOC removal efficiency were determined. The water samples were taken from ML-GFW with an initial pH of 9.7, and the results are shown in Fig. 2(a). The removal efficiency of TOC increased rapidly with the increase in reaction time, especially during the first 3 h. The TOC removal efficiency reached to 41.2% at a reaction time of 3 h. The rate of increase subsequently slowed down and reached a constant.

An ideal TOC removal efficiency was achieved at the reaction time of 3 h, and the maximum removal efficiency of 47.5% was reached at 6 h, which was only 15.3% higher than that obtained at 3 h. Extending the reaction time to 6 h doubles the power consumption and increases the operating costs. Considering the economic efficiency, the optimal reaction time for the treatment of ML-GFW with the O_3/H_2O_2 process was thus determined to be 3 h. Despite the high salinity and high content of organic matter in the wastewater, the desirable performance was possible to be obtained, showing a feasibility of this process.

3.1.2 Effects of pH

The initial pH of the samples plays a vital role in the degradation of organic pollutants according to the literature (Kusic et al., 2006; Wang et al., 2019b). In this study, the removal efficiency of TOC in ML-GFW by the O_3/H_2O_2 process was investigated at pH of 4, 6, 8, 9.7 (pH of raw wastewater) and 12. The results are shown in Fig. 2(b). The TOC removal efficiency increased when the pH value was varied from 4.0 to 9.7. The TOC removal efficiency reached a maximum of 40.8% at pH of 9.7. However, the removal efficiency decreased to 37.1% as the pH value further increased to 12. The results show that a low or a high pH impairs the mineralization of organic compounds.

The reaction process for the degradation of organic matter by ozone can be grouped into two categories: direct oxidation of dissolved organics by ozone molecules and the indirect reaction of organics by ·OH generated by ozone decomposition (Kusic et al., 2006; Solmaz et al., 2012; Malik et al., 2020). The main path of degradation under an acidic condition is the direct oxidation process because ozone does not readily decompose to produce ·OH. According to Schulte et al. (1995), ozone has limited oxidation ability (E = 2.07 V), and its degradation efficiency is lower at this condition. On the other hand, the chloride ions (Cl^-) present in ML-GFW can react with O_3 (Eqs. (4) and (5)) in acidic solution, reducing the chance of ozone to oxidize organic contaminants (Levanov et al., 2019b).

$$O_3 + 2H^+ + 2Cl^- \rightarrow Cl_2 + O_2 + H_2O \quad (4)$$

$$Cl_2(aq) + Cl^-(aq) \leftrightarrow Cl_3^-(aq) \quad (5)$$

With the increase of pH, OH^- and H_2O_2 in the water promote ozone to produce a large amount of ·OH, which is more oxidative (Lin et al., 2009), according to Eqs. (6)–(8).

$$O_3 + OH^- \rightarrow HO_2^- + O_2 \quad (6)$$

$$H_2O_2 \leftrightarrow HO_2^- + H^+ \quad (7)$$

$$O_3 + HO_2^- \rightarrow \cdot OH + O_2 + \cdot O_2^- \quad (8)$$

However, it has been reported that Cl^- generally acts as a hydroxyl radical scavenger, and reacts with ·OH according to Eqs. (9)–(11) (Jayson et al., 1973; Liao et al., 2001), especially under acidic conditions, generating secondary free radicals like $HOCl\cdot^-$, $Cl\cdot$ and $Cl_2\cdot^-$.

$$\cdot OH + Cl^- \rightleftharpoons HOCl\cdot^- \quad (9)$$

$$k^+ = (4.3 \pm 0.4) \times 10^9\ L/(mol \cdot s),$$

$$k^- = (6.1 \pm 0.8) \times 10^9 s^{-1}$$

$$HOCl\cdot^- + H^+ \rightleftharpoons H_2O + Cl\cdot \quad (10)$$

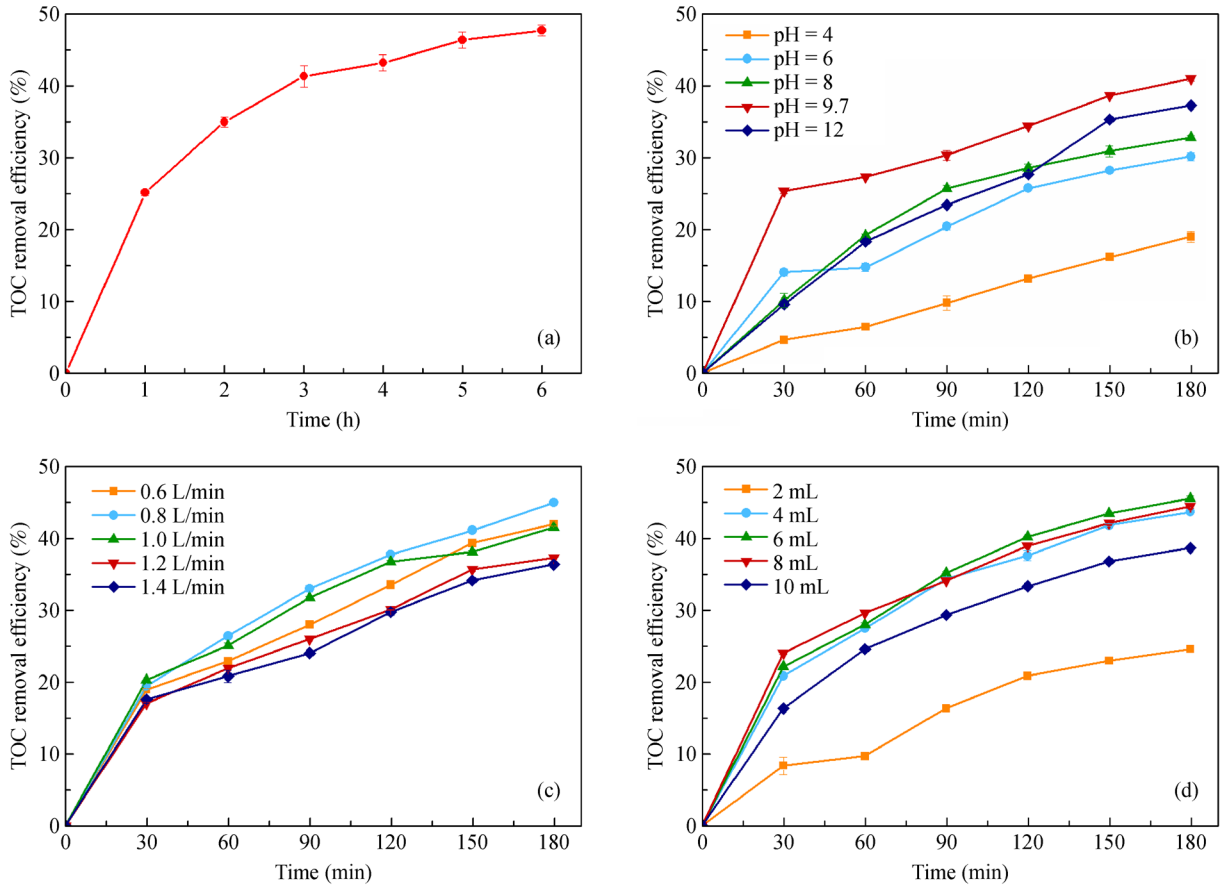

Fig. 2 The effects of (a) reaction time (pH = 9.7, ozone flow rate = 1 L/min, H_2O_2 dosage = 4 mL), (b) pH (reaction time = 180 min, ozone flow rate = 1 L/min, H_2O_2 dosage = 4 mL), (c) ozone flow rate (reaction time = 180 min, pH = 9.7, H_2O_2 dosage = 4 mL), (d) H_2O_2 dosage (reaction time = 180 min, pH = 9.7, ozone flow rate = 0.8 L/min) on TOC removal.

$$k^{+} = (2.1 \pm 0.7) \times 10^{10}\ \mathrm{L/(mol \cdot s)},$$

$$k^{-} = 1.3 \times 10^{3}\ \mathrm{s^{-1}}$$

$$\mathrm{Cl\cdot + Cl^{-} \rightleftharpoons Cl_2 \cdot^{-}} \qquad (11)$$

$$k^{+} = 2.1 \times 10^{10}\ \mathrm{L/(mol \cdot s)},$$

$$k^{-} = (1.1 \pm 0.4) \times 10^{5}\ \mathrm{s^{-1}}$$

These radicals have lower oxidation ability compared with ·OH, resulting in their poor reactivity to oxidize organic compounds. According to the results of Liao et al. (2001), the backward reaction in Eq. (9) occurs when pH is higher than 7.2, promoting the regeneration of ·OH. Thus, the indirect oxidation of organic contaminants could be adopted to improve the removal efficiency of TOC. When the initial pH was as high as 12, the decrease in removal efficiency was possibly due to the consumption of excessive ·OH. The excessive ·OH existing in the solutions reacts with $\cdot HO_2$ or itself to produce H_2O and O_2, resulting in a poor treatment performance.

The pH of the raw ML-GFW was 9.7, which is conducive to counteracting the side effects of the chloride ions. In summary, the effective initial pH for the pretreatment of ML-GFW with the O_3/H_2O_2 process was determined to be 9.7.

3.1.3 Effects of ozone flow rate

It has been widely accepted that the ozone flow rate (L/min or m^3/h) can be used as the unit to measure the ozone quantity in practical engineering applications. The amount of ozone molecules in the reaction system (ozone dosage) is determined by the ozone flow rate under a fixed reaction time, which in turn directly affects the TOC removal efficiency.

The effects of ozone flow rate on TOC removal with O_3/H_2O_2 process were hence evaluated in this study. Figure 2(c) demonstrates a significant influence of ozone flow rate on the treatment effect. The removal efficiency of TOC increased with the ozone flow rate increasing from 0.6 L/min to 0.8 L/min. And the maximum efficiency of 44.9% was obtained at an ozone flow rate of 0.8 L/min.

However, with a further increase in the ozone flow rate, the TOC removal efficiency decreased. The removal efficiency was only 36.3% at the biggest ozone flow rate of 1.4 L/min.

As the ozone flow rate is below 0.8 L/min, more ozone molecules are fed to the system due to the increase of ozone flow rate, enhancing the production of ·OH. This improves the removal effect. There was a slight increase in the ozone dosage with a further increase of ozone flow rate, possibly due to its saturation in aqueous. A faster flow rate may not allow enough time for gas and liquid to react completely, hindering the dissolution of ozone. Besides, an excessive amount of ozone becomes the scavenger of ·OH (Eq. (12)) (Ku et al., 1996; Kusic et al., 2006), resulting in a decreased removal efficiency.

$$\cdot OH + O_3 \rightarrow \cdot HO_2 + O_2 \quad (12)$$

The results indicate that the ozone flow rate is one of the key parameters for the mineralization of organic contaminants. Considering all of the factors mentioned above, such as the gas-liquid contact period, removal efficiency and operation costs, the optimal ozone flow rate was determined to be 0.8 L/min for the treatment of ML-GFW with O_3/H_2O_2 process.

3.1.4 Effects of H_2O_2 dosage

A single O_3 process was performed in the pre-experiment, but very low removal efficiency was obtained. After the addition of H_2O_2 in the treatment procedure, the removal efficiency improved significantly. It has already been reported that different dosages of H_2O_2 showed variable influences on the O_3/H_2O_2 process (Staehelin and Hoigne, 1982; Schulte et al., 1995; Arslan et al., 1999; Solmaz et al., 2012). In this study, the removal effect of TOC in ML-GFW with the O_3/H_2O_2 process was investigated as the dosage of H_2O_2 was varied from 2 mL to 10 mL. Figure 2(d) illustrates an initial increase in the efficiency followed by a subsequent decrease with the increasing dosage of H_2O_2. After reaction for 3 h, the highest efficiency of 45.4% was achieved at a dose of 6 mL.

The amount of hydroxyl radicals increases thanks to the increase of H_2O_2 dose ranging from 2 mL to 6 mL, enhancing the treatment efficiency. The continued increase in the H_2O_2 dosage declines the effectiveness of TOC removal. This might be the result of the scavenging reaction by the excessive H_2O_2, as shown in Eqs. (13) and (14) (Arslan et al., 1999). Besides, a high level of ·OH concentration brings about its self-quenching (Eq. (15)), hindering its reaction with organic contaminants in ML-GFW. All the aforementioned reactions result in a lower amount of ·OH in the system, decreasing the removal efficiency.

$$H_2O_2 + \cdot OH \rightarrow H_2O + \cdot HO_2 \quad (13)$$

$$HO_2^- + \cdot OH \rightarrow OH^- + \cdot HO_2 \quad (14)$$

$$4HO\cdot \rightarrow 2H_2O + O_2 \quad (15)$$

To sum up, the excessive H_2O_2 present in the system will not only reduce the removal efficiency of the process but also increase the operating costs. The optimal dosage of H_2O_2 for the treatment of ML-GFW with the O_3/H_2O_2 process was thus determined to be 6 mL.

To further improve the efficiency of removal of TOC, the dosing mode of equivalent H_2O_2 was investigated. H_2O_2 (6 mL) was divided into several parts and added at equal intervals during the reaction. When H_2O_2 was added separately at the beginning and midpoint of the reaction, the removal efficiency significantly increased from 45.8% to 64.6%. This was probably due to a more adequate progress of oxidation. Further increase in dosing times hardly improved the treatment efficiency. Therefore, subsequent experiments were conducted where H_2O_2 was dosed in two steps (0 min and 90 min). It was in favor of the effective utilization of H_2O_2 and was apt to operate.

3.2 RSM optimization experiments

3.2.1 Prediction model analysis

The single factor experiments demonstrated that a reaction time of 3 h, a pH value of 9.7, an ozone flow rate of 0.8 L/min, and the H_2O_2 dosage of 6 mL were the appropriate parameters. With the TOC removal efficiency as the response value, a central composite experiment (CCD) with three significant factors (pH, ozone flow rate, and H_2O_2 dosage) and five levels was designed (Table 1). A total of 20 sets of experiments were carried out, and the reaction time was 3 h for each experimental condition (Table 2).

Table 1 Factors and levels of RSM experiment (CCD)

Factors	Levels				
	$-\alpha$	−1	0	+1	$+\alpha$
pH	6.64	8.00	10.00	12.00	13.36
Ozone flow rate (L/min)	0.46	0.60	0.80	1.00	1.14
H_2O_2 dosage (mL)	2.64	4.00	6.00	8.00	9.36

A response surface analysis on the experimental data was performed using Design-expert 8.0.5. This gave the second-order polynomial model on TOC removal efficiency, as shown in Eq. (16).

$$Y = 73.53 + 9.47A + 1.40B + 1.73C - 1.60AB - 0.80AC + 1.13BC - 10.06A^2 - 4.65B^2 - 7.20C^2. \quad (16)$$

Table 2 The response of TOC removal efficiency of optimization experiments

Run	Factors			*Y*: TOC removal (%)
	A: pH	*B*: Ozone flow rate(L/min)	*C*: H_2O_2 dosage (mL)	
1	6.64	0.80	6.00	31.2
2	8.00	0.60	8.00	38.9
3	8.00	1.00	4.00	39.3
4	8.00	0.60	4.00	39.2
5	8.00	1.00	8.00	47.9
6	10.00	0.46	6.00	56.0
7	10.00	0.80	6.00	74.2
8	10.00	0.80	6.00	75.9
9	10.00	0.80	6.00	72.3
10	10.00	0.80	2.64	49.2
11	10.00	0.80	9.36	57.2
12	10.00	0.80	6.00	72.7
13	10.00	0.80	6.00	74.0
14	10.00	0.80	6.00	72.1
15	10.00	1.14	6.00	64.2
16	12.00	1.00	8.00	61.5
17	12.00	1.00	4.00	60.5
18	12.00	0.60	8.00	63.3
19	12.00	0.60	4.00	62.4
20	13.36	0.80	6.00	59.1

Here, *Y* represents the TOC removal efficiency (%), *A* represents the pH, *B* represents ozone flow rate, and *C* represents the H_2O_2 dosage.

ANOVA of this model is presented in Table 3. The *F*-value in the table presents the ratio of the model mean square deviation and its error. The *p*-value gives the probability of impossible events in the model. A large *F*-value and a small *p*-value indicate that the model has a strong significance to predict the outcomes better (Ghevariya et al., 2011). The *F*-value of the model was 81.29, and the *p*-value was < 0.0001, which confirmed that there was a good regression effect. The square of the complex

Table 3 ANOVA of the RSM model

Source	Sum of Squares	df [a)]	Mean Square	*F*-Value	*p*-Value Prob>F
Model	3480.38	9	386.71	81.29	< 0.0001
A	1224.73	1	1224.73	257.44	< 0.0001
B	27.14	1	27.14	5.71	0.0380
C	40.96	1	40.96	8.61	0.0149
AB	20.48	1	20.48	4.30	0.0648
AC	5.12	1	5.12	1.08	0.3240
BC	10.13	1	10.13	2.13	0.1753
A^2	1451.32	1	1451.32	305.07	< 0.0001
B^2	322.23	1	322.23	67.73	< 0.0001
C^2	744.82	1	744.82	156.56	< 0.0001
Residual	47.57	10	4.76		
Lack of Fit	37.04	5	7.41	3.52	0.0969
Pure Error	10.53	5	2.11		

Notes: a) df: degrees of freedom. Other values of ANOVA: Std. Dev.: 2.18, Mean: 58.56, *R*-Squared(R^2): 0.9865, Adj *R*-Squared(R_{adj}^2): 0.9744, Pred *R*-Squared (R_{pred}^2): 0.9117, Adeq Precision: 28.723, C.V. % (Coefficient of variance): 3.72, PRESS: 311.63.

correlation coefficient (R^2) of the model was calculated to be 0.9865, the square of the modified complex correlation coefficient (R_{adj}^2) was found to be 0.9744, and the square of the predicted complex correlation coefficient (R_{pred}^2) was determined to be 0.9117. All the values were greater than 0.8, and C.V.% was 3.72% ($< 10\%$), which further indicated a good fitting of the model (Sharma and Simsek, 2020). Adeq Precision characterizes the signal to noise ratio. A ratio greater than 4 is desirable, and a ratio of 28.723 in this study demonstrates an adequate signal. Consequently, this model can be utilized to conduct the design space.

Figure 3(a) presents the normal plot of residuals of the models with TOC removal efficiency as a response value. The linear distribution of each group of experimental results and the uniformly distributed data indicated that it was reasonable to take the TOC removal efficiency as the response value (Jing et al., 2017). The predicted and experimental values of the model illustrate a good agreement (Fig. 3(b)).

In conclusion, the model showed a desirable correlation between the response values and variables. The key parameters of ML-GFW treatment with the O_3/H_2O_2 process can be further optimized, and the TOC removal efficiency can be forecasted. The degree of influence of the three critical factors in the model was found to be: pH>H_2O_2 dosage>ozone flow rate. Compared with the interaction between the variables, the linear and square terms of the model were found to be more significant ($p < 0.05$). There are some interactions among the variables, which are specially discussed in the following section.

3.2.2 Interaction among crucial factors

The response surface plots and contour lines of the interaction of different factors on TOC removal efficiency were obtained using Design expert 8.0.5, as shown in Figs. 3(c)–3(h). In the 3D response surface plots, the steeper response surface shows a more significant effect on the response value (Sonwani et al., 2019). The darker color of the response surface indicates a higher TOC removal efficiency. The contour lines intuitively reflect the interaction and size of each factor, and the response surface plot corresponds to the contour lines. The closer the contour curve to the center, the higher the corresponding response value (Jiao et al., 2016).

It was observed that the slopes of the response surfaces became steeper, and the contour lines became denser from Figs. 3(c) and 3(d). It could be concluded that pH had a more significant influence than that of the ozone flow rate on TOC removal efficiency. This observation was consistent with the results of ANOVA. With the increase in ozone flow rate, the TOC removal efficiency initially increased, then tended to decrease at a constant pH value. Remarkably, an increase or decrease in the ozone flow rate did not effectively improve the removal efficiency at pH < 9. This was possibly due to the adverse effects of chloride ions under a low pH condition. At a fixed ozone flow rate, TOC removal efficiency increased steadily with the increase in the pH until it reached 11 then a slight decrease was observed. The maximum efficiency for TOC removal was obtained at a pH ranging from 10 to 12 and an ozone flow rate of 0.7 to 0.9 L/min. This has been represented in the darkest color on the response surface.

Figures 3(e) and 3(f) illustrate that the effect of H_2O_2 dosage on TOC removal efficiency is more conspicuous than that of ozone flow rate, which is in accordance with the results of ANOVA. Irrespective of whether the dosage of H_2O_2 was less than 4.5 mL or more than 7.5 mL, adjusting the ozone flow rate makes little difference on the TOC removal efficiency. When the dosage of H_2O_2 varied in the range of 5–7 mL, an increase in the ozone flow rate resulted in surface color of an initial dark and subsequent light. Correspondingly, the TOC removal efficiency first increased and then decreased with a slight variation. The TOC removal efficiency showed a trend of increasing at first and then declining with the increase in the H_2O_2 dosage at a fixed ozone flow rate. The best removal performance could be achieved at a dosage of H_2O_2 varying from 5.5 mL to 6.5 mL and an ozone flow rate of 0.7 to 0.9 L/min.

Compared with the H_2O_2 dosage, the pH value shows a greater significance (Figs. 3(g) and 3(h)). A change in H_2O_2 dosage had little influence on treatment performance at pH < 9. The removal efficiency of TOC initially increased and then decreased with the increase in H_2O_2 dose at a fixed pH value in the range of 10–11. The maximum removal efficiency was reached when the pH value was between 10 and 11, and the H_2O_2 dosage was between 5.5 mL and 6.5 mL.

According to these results, the order of the interaction among the different factors could be suggested as A-B>B-C>A-C. However, the interactions between them were not significant enough in ANOVA (p-value>0.05). The presence of complex components and uncertain elements in actual ML-GFW might be the reason behind the lack of significance.

3.2.3 Parameter optimization and model verification

To obtain the maximum removal efficiency of TOC, the operation parameters were optimized by Design-expert 8.0.5. The optimal combination of parameters was a pH value of 10.9, an ozone flow rate of 0.8 L/min, and H_2O_2 dosage of 6.2 mL. This predicted combination gave the maximum removal efficiency of 75.9%. The experiments were repeated thrice to verify the accuracy of the predicted results under these conditions, and the average actual removal efficiency was found to be 72.3% with the TOC

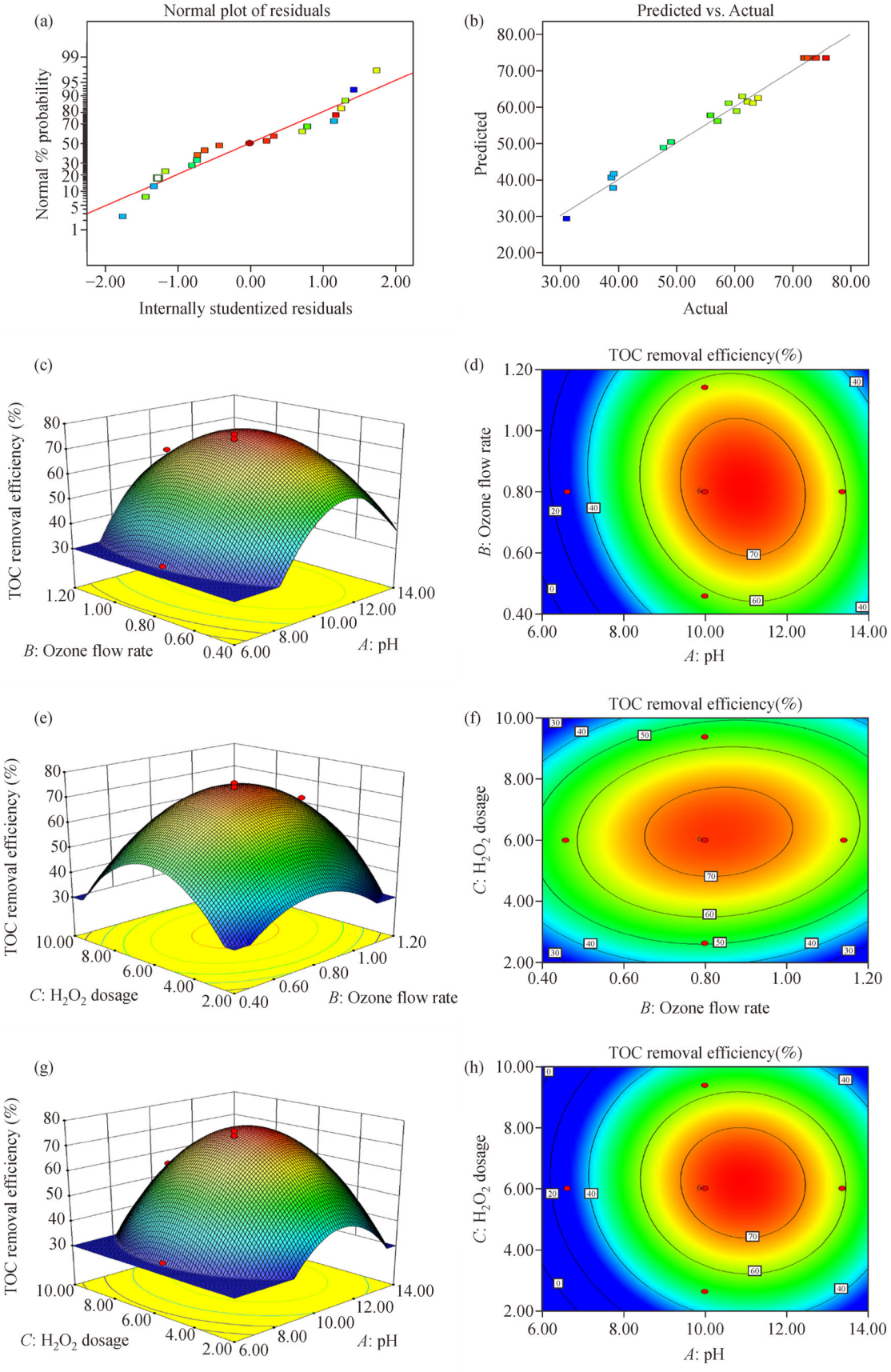

Fig. 3 Plots of RSM results ((a), (b)) and 3D response surface of combine effect of A-B ((c), (d)), B-C ((e), (f)), A-C ((g), (h)) on TOC removal efficiency.

concentration of 523 mg/L in the effluent. The measured value was close to the predicted value, with an acceptable relative standard deviation not exceeding 5%. Compared with the results of single-factor experiments (64.6%), the TOC removal efficiency after optimization with RSM (72.3%) was increased by 11.9%. The results showed that the RSM model was reliable for predicting the optimal operation conditions of actual wastewater treatment.

The successful prediction in this study indicates that the single-factor experiments are essential to determine the appropriate ranges and to improve the prediction accuracy.

3.3 Analysis of reaction mechanism

3.3.1 Ozone utilization experiments

Ozone is a common oxidant and has a strong oxidizing ability to degrade organic compounds. Its utilization rate is related to the removal efficiency of organic contaminants and the cost of operation. H_2O_2 is another powerful oxidant, and its oxidation mainly depends on its decomposition to produce ·OH. The addition of H_2O_2 in the ozone oxidation system could improve not only the utilization rate of ozone but also the removal rate of pollutants (Schulte et al., 1995; Arslan et al., 1999). H_2O_2 can react with O_3 as Eq. (17) (Kusic et al., 2006; Malik et al., 2020), promoting the production of ·OH that enhances the oxidizing ability of the system. Meanwhile, HO_2^- produced by the decomposition of a low concentration of H_2O_2 (Eq. (7)) accelerates the generation of ·OH (Eq. (8)). These processes are beneficial to the oxidation process, improving the removal efficiency of organic pollutants.

$$2O_3 + H_2O_2 \rightarrow 2 \cdot OH + 3O_2 \quad (17)$$

In order to verify that the addition of H_2O_2 improves the ozone utilization efficiency, the ozone utilization experiments under the predicted optimal conditions were carried out (Fig. 4(a)).

After the reaction was stable, the ozone utilization rate was calculated as 75% under the O_3/H_2O_2 process, while that under the single ozone process was only 48%. The results indicate the addition of H_2O_2 can effectively improve the utilization rate of ozone.

Notably, the dosage of ozone was calculated to be 9.84 mg O_3/mg TOC under the optimal operation conditions with an ozone utilization rate of 75%. The results obtained can potentially provide a useful reference for future practical applications.

3.3.2 Hydroxyl radical quenching experiments

Researchers used to qualitatively explain the existence and the generation mechanism of ·OH by adding hydroxyl radical scavenger to the reaction system. There are many kinds of hydroxyl radical quenchers, such as the benzoic acid (Wang et al., 2017), phenol (Zhang et al., 2013), and alcohols (Hwang et al., 2010; Monteagudo et al., 2011), among which the alcohols are the most widely applied. Tert-butanol (TBA) is the most commonly used ·OH quencher, which can rapidly capture ·OH in water (Eqs. (18) and (19)) (Flyunt et al., 2003; Monteagudo et al., 2011). However, it is almost inert against ozone with such a low reaction rate constant of 1.0×10^{-3} L/(mol·s) (Flyunt et al., 2003).

$$(CH_3)_3COH + \cdot OH \rightarrow \cdot CH_2C(CH_3)_2OH + H_2O \quad (18)$$

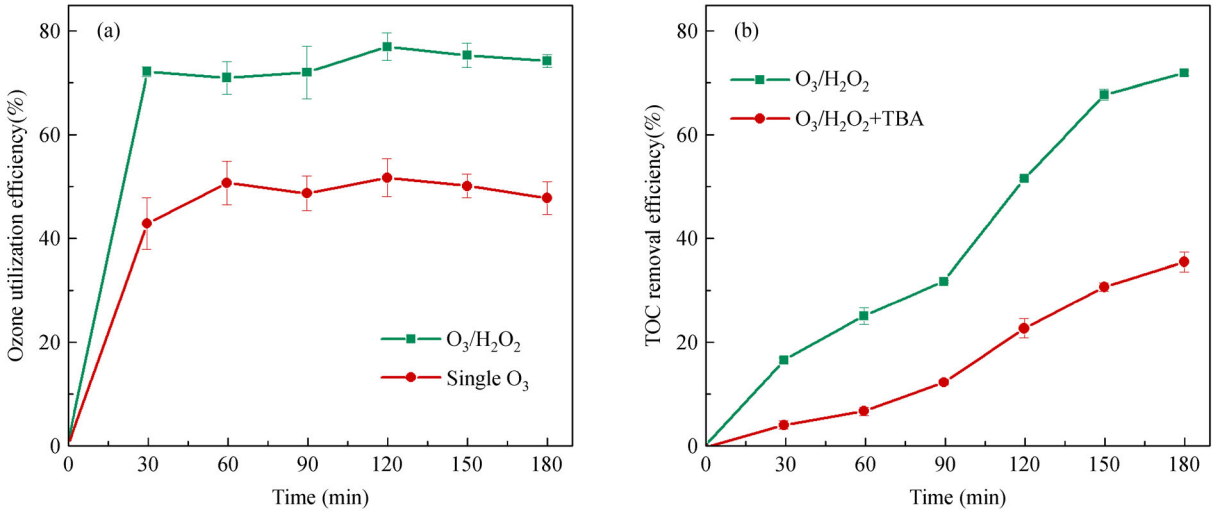

Fig. 4 Plots of mechanism verification experiments under optimized conditions (reaction time = 180 min, pH = 10.9, ozone flow rate = 0.8 L/min, H_2O_2 dosage = 6.2 mL): (a) the ozone utilization rate with O_3/H_2O_2 and single ozone process, (b) effect of TBA on TOC removal efficiency (TBA dosage = 15 mmol/L).

$$k = 6.0 \times 10^8 \mathrm{L/(mol \cdot s)}$$

$$(CH_3)_3COH + \cdot OH \rightarrow (CH_3)_2CO \cdot + H_2O \quad (19)$$

$$k = 6.0 \times 10^8 \mathrm{L/(mol \cdot s)}$$

In this study, TBA was added to quench ·OH under the optimal operating conditions of the O_3/H_2O_2 process to verify its dominant position in the oxidation process. The reaction was carried out for 3 h, and the results are presented in Fig. 4(b). After the addition of TBA, the removal efficiency of TOC decreased significantly to 35.6%, while that of the control group was as high as 71.8%. TBA scavenges most of the ·OH, reducing the chance of the reaction between ·OH and the contaminants. Besides, the intermediate products like $\cdot CH_2C(CH_3)_2OH$ and $(CH_3)_3CO\cdot$ generated during the reaction could further capture ·OH, causing a low removal efficiency of TOC.

The results of the quenching experiments indicated that hydroxyl radicals were generated abundantly during the treatment of ML-GFW with the O_3/H_2O_2 process, which contributed to the mineralization of organic matter.

3.4 Analysis of organic compounds

A desirable TOC removal efficiency of 72.3% was obtained under the optimized conditions, indicating that the O_3/H_2O_2 process can effectively mineralize most of the organic matter in actual ML-GFW. To investigate the specific degradation functions of the organics, the influents and effluents were analyzed by GC-MS, respectively. Figure 5 shows the results of GC-MS.

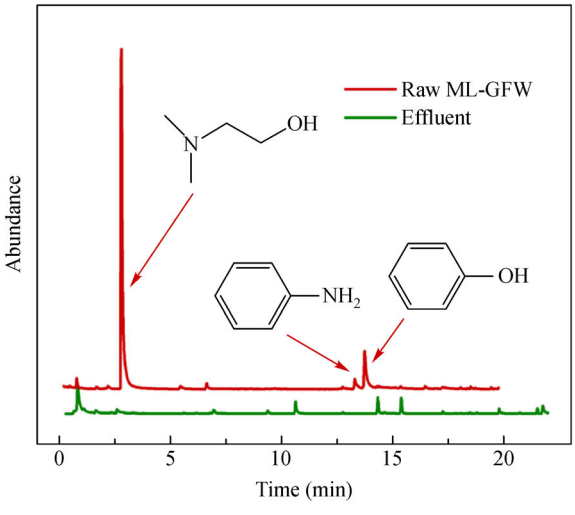

Fig. 5 Results of analysis of organic compounds by GC-MS.

The results show that the primary organic contaminant in ML-GFW is $C_4H_{11}NO$ (N, N-Dimethylethanolamine), the peak area of which was up to 82.88%. The secondary contaminants are phenol and aniline, and other pollutants including macromolecular organic matters, are also present in the raw ML-GFW. After carrying out the reaction for 3 h, the amount and height of peak detected in the effluent descended significantly, demonstrating an efficient degradation by the O_3/H_2O_2 process. However, a small amount of macromolecular organic compounds were still detected in the effluent, which probably were the intermediate product generated during the oxidation progress. Based on the GC-MS results, the possible degradation pathways of the primary contaminants are given in Fig. 6.

Some haloalkanes like dichloromethane (CH_2Cl_2), trichloromethane ($CHCl_3$), and tribromomethane ($CHBr_3$) were detected in the effluent, as a part of Cl^- and Br^- were oxidized into active halogen. They probably took part in the oxidation reaction when there was a slight decrease in the pH during the degradation process. The amount of chloride ions in the effluent was measured as about 95% of that in raw ML-GFW, further indicating that Cl^- had been involved in a certain way. This part of consumed chloride ion may be transferred into the organic phase (intermediate) or the inorganic phase (ClO^-, ClO_3^-) (Levanov et al., 2019a). The results obtained from GC-MS showed that further studies on the degradation of residual organic compounds are necessary to understand the reaction pathway.

4 Conclusions

The O_3/H_2O_2 process was adopted to pretreat the mother liquor of gas field wastewater (ML-GFW). Satisfactory results were achieved despite the high salinity of the raw wastewater. The response surface methodology (RSM) was successfully utilized to optimize the treatment parameters. The actual removal efficiency of TOC under the optimized conditions (reaction time = 180 min, pH = 10.9, ozone flow rate = 0.8 L/min, H_2O_2 dosage = 6.2 mL, and dosing H_2O_2 in two steps) was 72.3%, which deviated slightly from the predicted value. The results proved the reliability of the prediction model. The ozone dosage was calculated to be 9.84 mg O_3/mg TOC. The pH value was found to play a vital role in this process. Keeping an appropriate pH was conducive to the decomposition of ozone and alleviating the adverse effects of chloride ions. The primary selection of the critical factors and their ranges was based on singe-factor experiments that improved the success rate of the RSM prediction. Through the verification experiments and GC-MS analysis, it was observed that the synergistic effect of H_2O_2 and O_3 promoted the generation of hydroxyl radicals, achieving the degradation of most of the organic matter. This study provided the required data and technical supports for future research on treating ML-GFW.

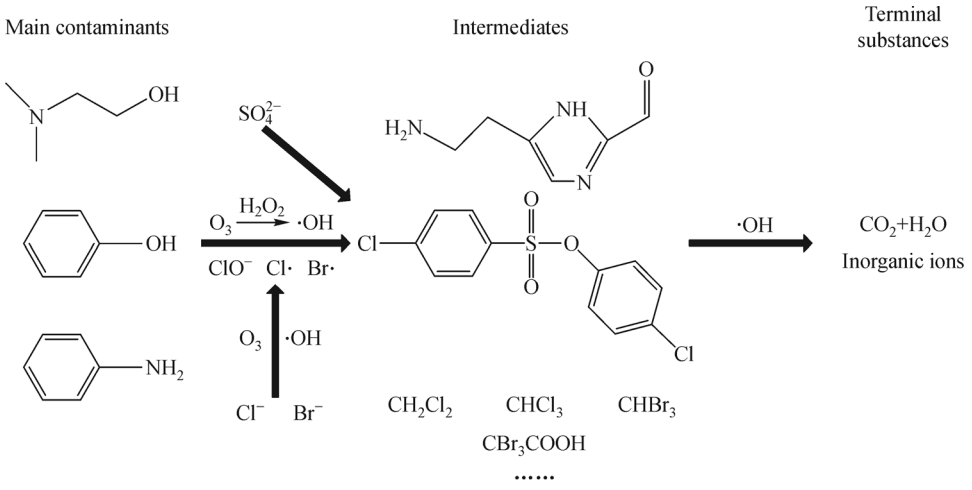

Fig. 6 Possible degradation pathways of main contaminants.

Acknowledgements This study was supported by the National Science and Technology Major Project of the 13th Five-Year Plan "High-efficiency development of ultra-deep bio-herm gas reservoirs with bottom water" (No. 2016ZX05017-005).

References

Arslan I, Balcioglu I A, Tuhkanen T (1999). Advanced oxidation of synthetic dyehouse effluent by O_3, H_2O_2/O_3 and H_2O_2/UV processes. Environmental Technology, 20(9): 921–931

Barndõk H, Hermosilla D, Cortijo L, Negro C, Blanco Á (2012). Assessing the effect of inorganic anions on TiO_2-photocatalysis and ozone oxidation treatment efficiencies. Journal of Advanced Oxidation Technologies, 15(1): 125–132

Cristóvão R O, Gonçalves C, Botelho C M, Martins R J E, Loureiro J M, Boaventura R A R (2015). Fish canning wastewater treatment by activated sludge: Application of factorial design optimization. Water Resources and Industry, 10: 29–38

Dai J X, Ni Y Y, Qin S F, Huang S P, Peng W L, Han W X (2018). Geochemical characteristics of ultra-deep natural gas in the Sichuan Basin, SW China. Petroleum Exploration and Development, 45(4): 619–628

Flyunt R, Leitzke A, Mark G, Mvula E, Reisz E, Schick R, von Sonntag C (2003). Determination of •OH, O_2•$^-$, and hydroperoxide yields in ozone reactions in aqueous solution. Journal of Physical Chemistry B, 107(30): 7242–7253

Fu P F, Lin X F, Li G, Chen Z H, Peng H (2018). Degradation of thiol collectors using ozone at a low dosage: Kinetics, mineralization, ozone utilization, and changes of biodegradability and water quality Parameters. Minerals (Basel), 8(11): 477

Ghevariya C M, Bhatt J K, Dave B P (2011). Enhanced chrysene degradation by halotolerant Achromobacter xylosoxidans using Response Surface Methodology. Bioresource Technology, 102(20): 9668–9674

Hwang S, Huling S G, Ko S (2010). Fenton-like degradation of MTBE: Effects of iron counter anion and radical scavengers. Chemosphere, 78(5): 563–568

Jayson G G, Parsons B J, Swallow A J (1973). Some simple, highly reactive, inorganic chlorine derivatives in aqueous solution. Their formation using pulses of radiation and their role in the mechanism of the Fricke dosimeter. Journal of the Chemical Society-Faraday Transactions 1, 69: 1597–1607

Jiao W Z, Yu L S, Feng Z R, Guo L, Wang Y H, Liu Y Z (2016). Optimization of nitrobenzene wastewater treatment with O_3/H_2O_2 in a rotating packed bed using response surface methodology. Desalination and Water Treatment, 57(42): 19996–20004

Jing L, Chen B, Wen D Y, Zheng J S, Zhang B Y (2017). Pilot-scale treatment of atrazine production wastewater by UV/O_3/ultrasound: Factor effects and system optimization. Journal of Environmental Management, 203: 182–190

Karimifard S, Moghaddam M R A (2018). Application of response surface methodology in physicochemical removal of dyes from wastewater: A critical review. Science of the Total Environment, 640: 772–797

Ku Y, Su W J, Shen Y S (1996). Decomposition kinetics of ozone in aqueous solution. Industrial & Engineering Chemistry Research, 35 (10): 3369–3374

Kusic H, Koprivanac N, Bozic A L (2006). Minimization of organic pollutant content in aqueous solution by means of AOPs: UV- and ozone-based technologies. Chemical Engineering Journal, 123(3): 127–137

Levanov A V, Isaikina O Y, Gasanova R B, Uzhel A S, Lunin V V (2019a). Kinetics of chlorate formation during ozonation of aqueous chloride solutions. Chemosphere, 229: 68–76

Levanov A V, Isaikina O Y, Lunin V V (2019b). Kinetics and mechanism of ozone interaction with chloride ions. Russian Journal of Physical Chemistry A, 93(9): 1677–1685

Li G J, He J J, Wang D D, Meng P P, Zeng M (2015). Optimization and interpretation of O_3 and O_3/H_2O_2 oxidation processes to pretreat hydrocortisone pharmaceutical wastewater. Environmental Technology, 36(8): 1026–1034

Liao C H, Kang S F, Wu F A (2001). Hydroxyl radical scavenging role of chloride and bicarbonate ions in the H_2O_2-UV process. Chemosphere, 44(5): 1193–1200

Lin C C, Chao C Y, Liu M Y, Lee Y L (2009). Feasibility of ozone absorption by H_2O_2 solution in rotating packed beds. Journal of Hazardous Materials, 167(1–3): 1014–1020

Lu T, Chen Y, Liu M, Jiang W J (2019). Efficient degradation of evaporative condensing liquid of shale gas wastewater using O_3/UV process. Process Safety and Environmental Protection, 121: 175–183

Malik S N, Ghosh P C, Vaidya A N, Mudliar S N (2020). Hybrid ozonation process for industrial wastewater treatment: Principles and applications: A review. Journal of Water Process Engineering, 35: 101193

Monteagudo J M, Durán A, San Martin I, Carnicer A (2011). Roles of different intermediate active species in the mineralization reactions of phenolic pollutants under a UV-A/C photo-Fenton process. Applied Catalysis B: Environmental, 106: 242–249

Moradi M, Vasseghian Y, Khataee A, Kobya M, Arabzade H, Dragoi E-N (2020). Service life and stability of electrodes applied in electrochemical advanced oxidation processes: A comprehensive review. Journal of Industrial and Engineering Chemistry, 87: 18–39

Oh B T, Seo Y S, Sudhakar D, Choe J H, Lee S M, Park Y J, Cho M (2014). Oxidative degradation of endotoxin by advanced oxidation process (O_3/H_2O_2 & UV/H_2O_2). Journal of Hazardous Materials, 279: 105–110

Ozgun H, Ersahin M E, Erdem S, Atay B, Sayili S, Eren E, Hoshan P, Atay D, Altinbas M, Kinaci C, Koyuncu I (2013). Comparative evaluation for characterization of produced water generated from oil, gas, and oil-gas production fields. CLEAN- Soil Air Water, 41(12): 1175–1182

Schulte P, Bayer A, Kuhn F, Luy T, Volkmer M (1995). H_2O_2/ O_3, H_2O_2/ UV and H_2O_2/ Fe^{2+} processes for the oxidation of hazardous wastes. Ozone: Science & Engineering, 17(2): 119–134

Sharma S, Simsek H (2020). Sugar beet industry process wastewater treatment using electrochemical methods and optimization of parameters using response surface methodology. Chemosphere, 238: 124669

Solmaz S K, Azak H, Morsunbul T (2012). A comparative study of the removal of 3-indolebutyric acid using advanced oxidation processes. Water Environment Research, 84(2): 100–107

Sonwani R K, Swain G, Giri B S, Singh R S, Rai B N (2019). A novel comparative study of modified carriers in moving bed biofilm reactor for the treatment of wastewater: Process optimization and kinetic study. Bioresource Technology, 281: 335–342

Staehelin J, Hoigne J (1982). Decomposition of ozone in water-rate of initiation by hydroxide ions and hydrogen peroxide. Environmental Science & Technology, 16(10): 676–681

Wang X M, Li N, Li J Y, Feng J J, Ma Z, Xu Y T, Sun Y C, Xu D M, Wang J, Gao X L, Gao J (2019a). Fluoride removal from secondary effluent of the graphite industry using electrodialysis: Optimization with response surface methodology. Frontiers of Environmental Science & Engineering, 13(4): 51

Wang Y, Li H Q, Ren L M (2019b). Organic matter removal from mother liquor of gas field wastewater by electro-Fenton process with the addition of H_2O_2: effect of initial pH. Royal Society Open Science, 6 (12): 191304

Wang Y, Lin X H, Shao Z Z, Shan D P, Li G Z, Irini A (2017). Comparison of Fenton, UV-Fenton and nano-Fe_3O_4 catalyzed UV-Fenton in degradation of phloroglucinol under neutral and alkaline conditions: Role of complexation of Fe^{3+} with hydroxyl group in phloroglucinol. Chemical Engineering Journal, 313: 938–945

Wen G, Ma J, Liu Z Q, Zhao L (2011). Ozonation kinetics for the degradation of phthalate esters in water and the reduction of toxicity in the process of O_3/H_2O_2. Journal of Hazardous Materials, 195: 371–377

Wu X Q, Liu G X, Liu Q Y, Liu J D, Yuan X Y (2016). Geochemical characteristics and genetic types of natural gas in the Changxing-Feixianguan Formations from the Yuanba Gas Field in the Sichuan Basin, China. Journal of Natural Gas Geoscience, 1(4): 267–275

Yang J, Xiang Q G (2018). New progress in wastewater treatment technology for standard-reaching discharge in sour gas fields. Natural Gas Industry B, 5(1): 75–79

Yazici Guvenc S, Varank G (2021). Degradation of refractory organics in concentrated leachate by the Fenton process: Central composite design for process optimization. Frontiers of Environmental Science & Engineering, 15(1): 2

Zhang J, Shao X T, Shi C, Yang S Y (2013). Decolorization of Acid Orange 7 with peroxymonosulfate oxidation catalyzed by granular activated carbon. Chemical Engineering Journal, 232: 259–265